THE JOURNAL OF BIOLOGICAL CHEMISTRY VOL. 281, NO. 10, pp. 6874–6883, March 10, 2006
Printed in the U.S.A.

The Rab5 Guanine Nucleotide Exchange Factor Rabex-5 Binds Ubiquitin (Ub) and Functions as a Ub Ligase through an Atypical Ub-interacting Motif and a Zinc Finger Domain*

Received for publication, September 9, 2005, and in revised form, December 8, 2005 Published, JBC Papers in Press, January 5, 2006, DOI 10.1074/jbc.M509939200

Rafael Mattera[‡], Yien Che Tsai[§], Allan M. Weissman[§], and Juan S. Bonifacino[‡1]

From the [‡]Cell Biology and Metabolism Branch, NICHD, National Institutes of Health, Bethesda, Maryland 20892 and the [§]Laboratory of Protein Dynamics and Signaling, NCI-Frederick, National Institutes of Health, Frederick, Maryland 21702

Rabex-5, the mammalian orthologue of yeast Vps9p, is a guanine nucleotide exchange factor for Rab5. Rabex-5 forms a tight complex with Rabaptin-5, a multivalent adaptor protein that also binds to Rab4, Rab5, and to domains present in γ-adaptins and the Golgi-localized, γ-ear-containing, ARF-binding proteins (GGAs). Rabaptin-5 augments the Rabex-5 exchange activity, thus generating GTP-bound, membrane-associated Rab5 that, in turn, binds Rabaptin-5 and stabilizes the Rabex-5·Rabaptin-5 complex on endosomes. Although the Rabex-5·Rabaptin-5 complex is critical to the regulation of endosomal fusion, the structural determinants of this interaction are unknown. Likewise, the possible binding and covalent attachment of ubiquitin to Rabex-5, two modifications that are critical to the function of yeast Vps9p in endosomal transport, have not been studied. In this study, we identify the 401–462 and 551–661 coiled-coils as the regions in Rabex-5 and Rabaptin-5, respectively, that interact with one another. We also demonstrate that Rabex-5 undergoes ubiquitination and binds ubiquitin, though not via its proposed C-terminal CUE-like domain. Instead, the N-terminal region of Rabex-5 (residues 1–76), comprising an A20-like Cys_2/Cys_2 zinc finger and an adjacent α-helix, is important for ubiquitin binding and ubiquitination. Importantly, we demonstrate that the Rabex-5 zinc finger displays ubiquitin ligase (E3) activity. These observations extend our understanding of the regulation of Rabex-5 by Rabaptin-5. Moreover, the demonstration that Rabex-5 is a ubiquitin ligase that binds ubiquitin and undergoes ubiquitination indicates that its role in endosome fusion may be subject to additional regulation by ubiquitin-dependent modifications.

Rabex-5, the mammalian orthologue of yeast Vps9p, is a guanine nucleotide exchange factor (GEF)[2] that catalyzes the exchange of GTP for GDP on the Rab5 subfamily of low molecular weight GTPases composed of Rab5, Rab21, and Rab22 (1–3). Secondary structure predictions and x-ray crystallographic analyses have shown that Rabex-5 comprises several structural elements and domains, including an A20-like Cys_2/Cys_2 zinc finger (ZnF) followed by an α-helix, a triple α-helical bundle, a Vps9 domain that possesses the GEF activity, a coiled-coil, and a proline-rich C-terminal extension (3) (Fig. 1*A*). Rabex-5 forms a tight complex with Rabaptin-5, a multivalent adaptor protein that contains independent binding sites for Rab4 (4), Rab5 (4), the γ-adaptin ear (GAE) domains of γ-adaptins and Golgi-localized, γ-ear-containing, ARF-binding proteins (GGAs) (5) and the GGAs and TOM1 (GAT) domains of GGA1 and GGA2 (5, 6) (Fig. 1*B*).

The binding of Rabaptin-5 increases the GEF activity of Rabex-5 and accelerates the generation of the active GTP-bound form of membrane-associated Rab5, which, in turn, binds to Rabaptin-5 (2). Thus, the Rabex-5·Rabaptin-5 complex has properties of both a GEF and an effector for Rab5. The resulting tripartite interaction is believed to stabilize a fraction of the cytosolic Rabex-5·Rabaptin-5 complex on endosomes, thus amplifying the generation of GTP-bound Rab5 and leading to enhanced endosome fusion (1, 2). The binding of ubiquitin (Ub) and the ubiquitination of target proteins are also critical events in endocytosis, endosomal sorting, and endosome fusion (7–9). For instance, the activity of yeast Vps9p is regulated by Ub binding and covalent monoubiquitination of this protein, both of which depend on a C-terminal CUE1p homologous (CUE) domain (10–12). On the basis of sequence homology, mammalian Rabex-5 was proposed to contain a domain analogous to CUE at its C terminus (10), but the Ub binding activity of this domain was not examined.

Despite the critical requirement of the Rabaptin-5 interaction for Rabex-5 GEF activity and endosome fusion, the structural determinants responsible for this interaction have not been identified. Likewise, the possible interaction of Rabex-5 with Ub and its ubiquitination have not been studied. In this study, we identify two coiled-coils comprising residues 401–462 and 551–661 in Rabex-5 and Rabaptin-5, respectively, as the elements that mediate the interaction between these two proteins. We also demonstrate that Rabex-5 undergoes ubiquitination and binds directly to Ub though not via its proposed CUE-like domain. Instead the N-terminal region of Rabex-5 (residues 1–76, comprising the A20-like ZnF domain and the adjacent α-helix) binds Ub *in vitro* and is also important for the *in vivo* ubiquitination of this protein. Importantly, we demonstrate that the A20-like ZnF domain displays Ub ligase (E3) activity. These observations identify the structural determinants responsible for the regulation of Rabex-5 by Rabaptin-5. Moreover, the demonstration that Rabex-5 is an Ub ligase (E3) that binds Ub and undergoes ubiquitination indicates that this key GEF in endosome fusion may be subject to regulation, not only by Rabaptin-5, but also through Ub-dependent interactions.

EXPERIMENTAL PROCEDURES

DNA Constructs

pGAD and pGBT9 Constructs—SacII-SpeI and NotI-SpeI fragments encoding full-length Rabex-5 excised from pGEM T-bovine

* This research was supported by the Intramural Research Programs of the NICHD and NCI, National Institutes of Health. The costs of publication of this article were defrayed in part by the payment of page charges. This article must therefore be hereby marked "*advertisement*" in accordance with 18 U.S.C. Section 1734 solely to indicate this fact.

[1] To whom correspondence should be addressed: Cell Biology and Metabolism Branch, NICHD, Bldg. 18T/Rm. 101, National Institutes of Health, Bethesda, MD 20892. Tel.: 301-496-6368; Fax: 301-402-0078; E-mail: juan@helix.nih.gov.

[2] The abbreviations used are: GEF, guanine nucleotide exchange factor; GST, glutathione *S*-transferase; AD, transcription activation domain; BD, DNA binding domain; CUE, Cue1p-homologous; GAE, γ-adaptin ear; GAT, domain found in GGAs and TOM1; GGA, Golgi-localized, γ-ear-containing, Arf-binding protein; Hrs, hepatocyte growth factor-regulated tyrosine kinase substrate; STAM; signal-transducing adaptor molecule; TGN, *trans*-Golgi network; TSG101; tumor susceptibility gene 101 product; Ub, ubiquitin; UIM, ubiquitin-interacting motif; VHS, Vps27, Hrs, Stam; Vps, vacuolar protein sorting; XIAP, X-linked inhibitor of apoptosis; ZF, zinc finger; HA, hemagglutinin.

Rabex-5 plasmid (Ref. 2, gift from Marino Zerial, Max Planck Institute, Dresden, Germany) were filled-in with T4 DNA polymerase and subcloned into pGAD424 and pGBT9 vectors (Clontech) previously digested with BamH1 and filled-in with T4 DNA polymerase. Ligation of the SacII-SpeI and NotI-SpeI fragments generated the extra N-terminal sequences GGGRSSP and GRSSP, respectively, preceding the Rabex-5 initiation codon. The pGAD424- and pGBT9-Rabaptin-5 constructs were described in Refs. 5 and 13. Substitutions in Rabaptin-5 and Rabex-5 were generated using the QuikChange site-directed mutagenesis kit (Stratagene, La Jolla, CA). This system was also used to generate the Rabex-5-(1–124), -(1–257), -(1–399), and -(1–460) deletion constructs (using primers introducing the desired stop codons), and the internal deletion constructs 1–76^126–460, 1–76^251–460, 1–76^400–460, and 13–49^400–460 (using primers linking the merged regions). The same mutagenesis kit was used to generate the pGAD424-Rabex-5 1–76^400–460 C19A/C23A/C35A/C38A mutant. The Rabex-5-(401–462), -(456–492), and -(401–492) constructs were prepared by PCR amplification using upstream and downstream primers containing EcoR1 and BamH1fragments, respectively, followed by subcloning into the corresponding sites of pGAD424 and pGBT9. The pGBT9-human ubiquitin construct was described in Ref. 13; the corresponding ΔG75/G76 mutant was generated using the QuikChange site-directed mutagenesis kit. The GGA1-VHS+GAT and GGA3-VHS+GAT constructs were described in Refs. 13 and 14, respectively.

GST Fusion Constructs—A GST-Rabex-5-(1–76)^(400–460) construct was generated by SmaI digestion of the corresponding pGAD424 construct followed by subcloning into the StuI site of pGST1 parallel (15). The pGST1 parallel Rabex-5-(1–49) and -(1–76) were generated by introducing the corresponding stop codons in GST-Rabex-5-(1–76)^(400–460) using the QuikChange site-directed mutagenesis kit. The same mutagenesis kit was used to generate the pGST1 parallel Rabex-5-(1–76) constructs encoding the W55A and A58D substitutions. The GST-β3B ear and GST-GGA1-VHS+GAT constructs were described in Ref. 13, and the GST-XIAP in Ref. 16.

Myc-tagged Constructs—An NcoI/PstI fragment obtained following digestion of pGEM-Myc-human-Rabaptin-5 (termed pGEM-MycUEP in Ref. 4) was filled in with T4-DNA-polymerase and ligated into SmaI-digested pCI-neo (Promega, Madison, WI) to generate pCI-neo-Myc-Rabaptin-5. This construct was digested with ApaI and NotI to release the insert, and the vector with the Myc tag was subsequently treated with T4 DNA polymerase. A SacII/SpeI fragment encoding Rabex-5 (excised from pGEM T-Rabex-5 and filled-in with T4-DNA polymerase) was subcloned into the blunt-ended pCI-neo-Myc fragment to generate pCI-neo-Myc-Rabex-5 (tagged at the N terminus of Rabex-5). This construct contained an extra GGGRSSP between the Myc tag and the start of the Rabex-5 coding sequence. Both the pCI-neo-Myc-Rabex-5 Δ13–49 and pCI-neo-Myc-Rabex-5 A58D mutants were obtained using the above described QuikChange site-directed mutagenesis kit. The pCI-neo-Myc-stonin 2 proline-rich domain was described in Ref. 17.

Antibodies

The goat anti-Rabaptin-5 antiserum (6162) was obtained from Santa Cruz Biotechnology, while the mouse monoclonal anti-Rabaptin-5 and anti-Rabex-5 antibodies were purchased from Transduction Laboratories (Lexington, KY). The monoclonal anti-Rabex-5 was raised using a C-terminal fragment (residues 426–481) as immunogen; this antibody does not bind to Rabex-5-(456–492) (results not shown), suggesting that it recognizes an epitope located in the 426–455 region. The mouse monoclonal anti-Myc and anti-HA antibodies were purchased from Invitrogen and Covance, respectively, whereas the polyclonal anti-Myc antiserum was from Cell Signaling. The rabbit anti-GST was described in Ref. 18, and the rabbit anti-Rabex-5 antiserum was a kind gift from Marino Zerial. The rabbit anti-Ub antiserum was described in Ref. 19.

Yeast Two-hybrid Analysis

The AH109 yeast reporter strain was maintained on YPD agar plates. Transformation of AH109 cells with pGAD424- and pGBT9-based constructs by the lithium acetate method was performed following the instructions for the Matchmaker two-hybrid system (Clontech). The plating of transformants and the positive and negative experimental controls are described in the legend to Fig. 2.

Pull-down Assays Using Ub-Agarose Beads

20-μl aliquots of washed Ub-agarose (Affinity Bioreagents, Golden, CO) or protein A-agarose (Sigma) were incubated for 3 h at 4 °C with 1.5 μg of the indicated GST fusion proteins in a final volume of 500 μl of 15 mM HEPES pH 7.0, 75 mM NaCl, and 0.25% Triton X-100 (binding buffer) supplemented with 0.15% bovine serum albumin and protease inhibitors (EDTA-free Complete, Roche Applied Science). At the end of this period, samples were washed three times by resuspension in 1.3 ml of binding buffer without bovine serum albumin and centrifugation for 2 min at 2,000 × *g* and 4 °C, followed by a final wash with phosphate-buffered saline under the same conditions. The GST fusion proteins bound to the washed beads were eluted by resuspension in 60 μl of 2× Laemmli buffer and incubation at 90 °C for 10 min. The eluted samples were separated by centrifugation for 2 min at 16,000 × *g*, and subjected to SDS-PAGE and immunoblotting with rabbit anti-GST antiserum.

Ubiquitination Assays in Transfected HeLa Cells

HeLa cells were plated on 100-mm culture dishes and grown to ~50% confluency at 37 °C in Dulbecco's modified Eagle's medium supplemented with 10% fetal bovine serum, 100 units/ml penicillin, and 100 mg/ml streptomycin under a humidified atmosphere (95:5 air/CO_2). Cells were subsequently transfected with 7.5 μg of pCI-neo-Myc-bovine Rabex-5 (wild type or mutant) or control constructs and 2.5 μg of pCI-neo-$(HA)_3$-human Ub using the Fugene™ reagent (Roche Applied Science) followed by addition of 5 mM sodium butyrate and incubation for an additional 12–15 h at 37 °C. In the experiments aimed at examining the ubiquitination of endogenous Rabex-5, cells were only transfected with 2.5 μg of pCI-neo-$(HA)_3$-human Ub. At the end of the 12–15-h incubation, cells were washed three times with phosphate-buffered saline and lysed in 1 ml of 50 mM Tris-HCl, pH 7.4, 75 mM NaCl, and 0.5% Triton X-100 (extraction buffer) supplemented with protease inhibitors (EDTA-free Complete, Roche Applied Science). After a 30-min extraction at 4 °C, the lysates were spun for 15 min at 16,000 × *g* and 4 °C, and the supernatants were subsequently precleared by treatment for 30 min at 4 °C with 25 μl of protein G-Sepharose and centrifugation for 2 min at 16,000 × *g*. The precleared extracts were supplemented with 1 mg of bovine serum albumin and subjected to immunoprecipitation by further incubation for 3 h at 4 °C with 2.5 μg of antibodies immobilized onto 25 μl of protein G-Sepharose. At the end of this period, samples were centrifuged for 2 min at 2,000 × *g* and 4 °C and washed (three times with extraction buffer containing 0.1% Triton X-100 and once with phosphate-buffered saline) by resuspension and immediate centrifugation under the same conditions. Proteins bound to washed beads were eluted as described for the Ub-agarose binding assays, and the eluted materials subjected to SDS-PAGE and immunoblotting.

E3 Activity Assay

Reaction mixtures contained 1 μM E3 enzymes fused to GST, 100 nM recombinant murine E1 (expressed in Sf9 cells), 150–200 nM human recombinant E2 (expressed in *Escherichia coli*), 10 μM Ub, 0.5–1 μM ubiquitin aldehyde in a final volume of 30 μl of 20 mM Tris-HCl, pH 7.5, 100 mM NaCl, 4 mM ATP, and 2 mM $MgCl_2$. Mixtures were incubated at 30 °C for 2 h and quenched with SDS sample buffer. Samples were subjected to SDS-PAGE and immunoblotting with rabbit anti-Ub antibody. In some experiments (Fig. 6*D*), the E3 activity was evaluated in assays using reaction mixtures and incubation conditions identical to those described above, except for the presence of ^{32}P-labeled Ub (0.02 μCi, representing 0.2–0.3 μM Ub) instead of 10 μM unlabeled Ub. At the end of the incubation, the radioactive samples were subjected to SDS-PAGE; the gels were subsequently dried, exposed to a phosphor screen and imaged in a Storm Phoshorimager (Molecular Dynamics). The E2 thiolester assays were performed using reaction mixtures identical to those in the E3 activity assays with ^{32}P-labeled Ub, except for the absence of E3 enzyme. Samples were incubated at 30 °C for 10 min and subsequently resuspended in non-reducing or reducing SDS sample buffer and subjected to SDS-PAGE and imaging. The ^{32}P-labeled Ub was prepared as described by Scheffner *et al.* (20); the recombinant E2 enzymes were prepared as described in Ref. 21.

RESULTS

Coiled-coil Interactions Mediate the Assembly of Rabex-5 with Rabaptin-5—The domain organization of Rabex-5 and Rabaptin-5, used as the basis for mutational analyses, is shown in Fig. 1. The structural determinants of the Rabex-5-Rabaptin-5 interaction were analyzed using the yeast two-hybrid system. The results shown in Fig. 2*A* demonstrate that the Rabaptin-5 C2–1 coiled-coil domain (551–661 fragment) is the minimal fragment that binds to full-length Rabex-5. Interestingly, the GGA1-GAT domain interacts with the N-terminal region of a parallel coiled-coil Rabaptin-5-(551–661) homodimer, whereas residues in the central to C-terminal region of this fragment are involved in the stabilization of a Rabaptin-5-(551–661) tetramer (6). Given these facts, we analyzed a series of Rabaptin-5-(551–661) mutants to determine whether the same residues that are involved in the binding to GGA1-GAT and/or in the stabilization of the Rabaptin-5-(551–661) tetramer also play a role in the assembly with Rabex-5. The substitutions introduced in Rabaptin-5-(551–661) included Q561A, L564A, Q566A (residues contacting GGA1-GAT) as well as L610A/L613A, L610W/L613W, and L617A (residues that presumably stabilize the homotetramer) (6). The results in Fig. 2*B* show that although the Rabaptin-5-(551–661) mutants Q561A and L564A are indeed unable to bind GGA1-GAT, they interact with Rabex-5 in a manner similar to that of the wild-type construct. In contrast, the Rabaptin-5-(551–661) L610W/L613W mutant exhibited severely reduced interaction with Rabex-5, whereas the L610A/L613A mutant showed a partial decrease and the L617A mutant displayed a normal interaction (Fig. 2*B*). Removal of a relatively mobile region at the C terminus of Rabaptin-5-(551–661) (6), generating the Rabaptin-5-(551–643) and Rabaptin-5-(551–648) fragments, did not affect the interaction with Rabex-5 (Fig. 2*B*). Finally, we also analyzed the Rabex-5 domains that are responsible for the interaction with Rabaptin-5-(551–661). The different Rabex-5 constructs used in this analysis, and also elsewhere in this study, are schematized in Fig. 1*A*. We found that the Rabex-5 coiled-coil (fragment 401–462) is both necessary and sufficient for the interaction with Rabaptin-5 (Fig. 2*C*). Taken together, these results identify the 401–462 and 551–661 coiled-coils in Rabex-5 and Rabaptin-5, respectively, as

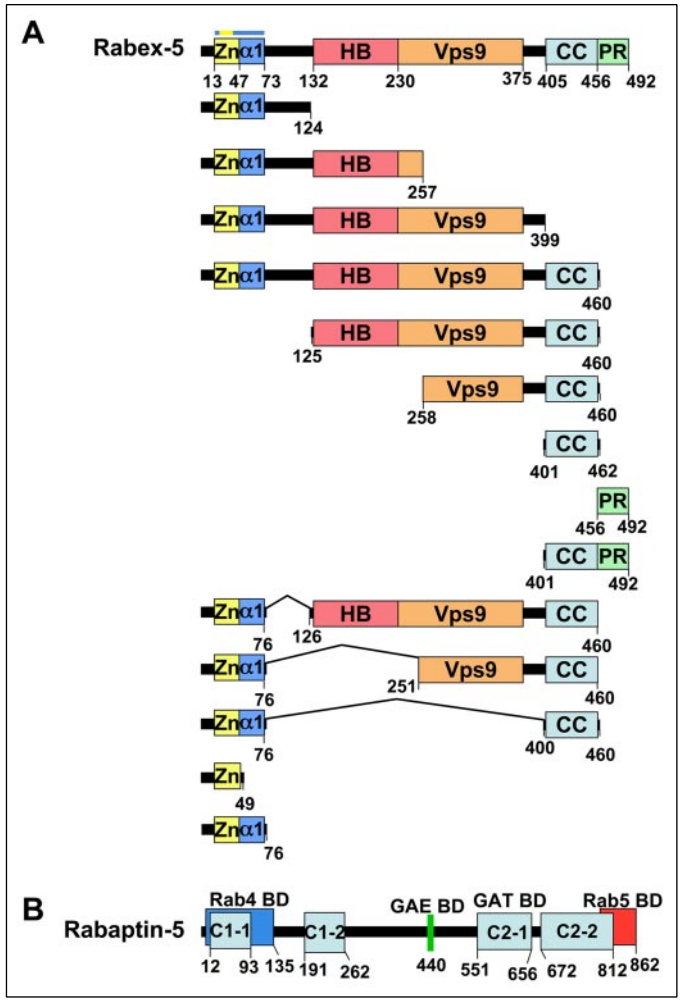

FIGURE 1. **Domains in Rabex-5 and Rabaptin-5 and scheme of constructs used in this study.** *A*, Rabex-5 Cys_2/Cys_2 ZnF domain with an 11-residue loop (labeled as *Zn*) and the adjacent α-helical region (α1) are portrayed as a *yellow-blue* tandem. The *yellow* portion of the bar above the Zn-α1 tandem represents the exact length of the finger (random coil structure from Cys^{19} to Cys^{38}), which is preceded by a short α-helix and is followed by the α1-helix (*blue portion of the bar*). The Rabex-5 Vps9 domain, and the helical bundle (*HB*) that stabilizes it, are defined according to Delprato *et al.* (3). Other relevant regions in Rabex-5 include the heptad repeats characteristic of coiled-coils (defined using the Network Protein Sequence Analysis, Pole Bioinformatique Lyonnais; Ref. 35) and the C-terminal proline-rich (*PR*) region. The different Rabex-5 constructs used in this study are also schematized in this panel. The numbering shown corresponds to the bovine Rabex-5 sequence used in this study. *B*, relevant modules in the Rabaptin-5 molecule include the binding domains for Rab4 and Rab5 (Rab4 BD and Rab5 BD; Ref. 4) and for the GAE domains of γ-adaptins and GGAs and the GAT domains of GGA1 and GGA2 (GAE BD and GAT BD, respectively; Ref. 5). The four regions containing heptad repeats characteristic of α-helical coiled-coils in Rabaptin-5 are designated as C1-1, C1-2, C2-1, and C2-2 (4). The numbering shown corresponds to the human Rabaptin-5 sequence.

the regions that drive the formation of the Rabex-5·Rabaptin-5 complex.

Rabex-5 Interacts with Ubiquitin Independently of Its Putative CUE Domain—We recently reported the binding of GGA1, Rabaptin-5, and Rabex-5 from a cell extract to Ub-agarose (13). Because GGA1 directly binds Ub via its GAT domain (13, 22), and the Rabex-5·Rabaptin-5 complex binds GGA1 (5), the interaction of the Rabex-5·Rabaptin-5 complex with Ub could be direct or indirect. The nature of these interactions was analyzed with the yeast two-hybrid system. The analysis showed that Rabaptin-5 does not interact with Ub, whereas Rabex-5 does so with an avidity that is intermediate between those of the VHS+GAT constructs of GGA1 and GGA3 (Fig. 3*A*). Recent reports indicate that Vps9p, the yeast ortholog of Rabex-5, binds Ub through its C-terminal Cue1p-homologous (CUE) domain, a tri-helical region that

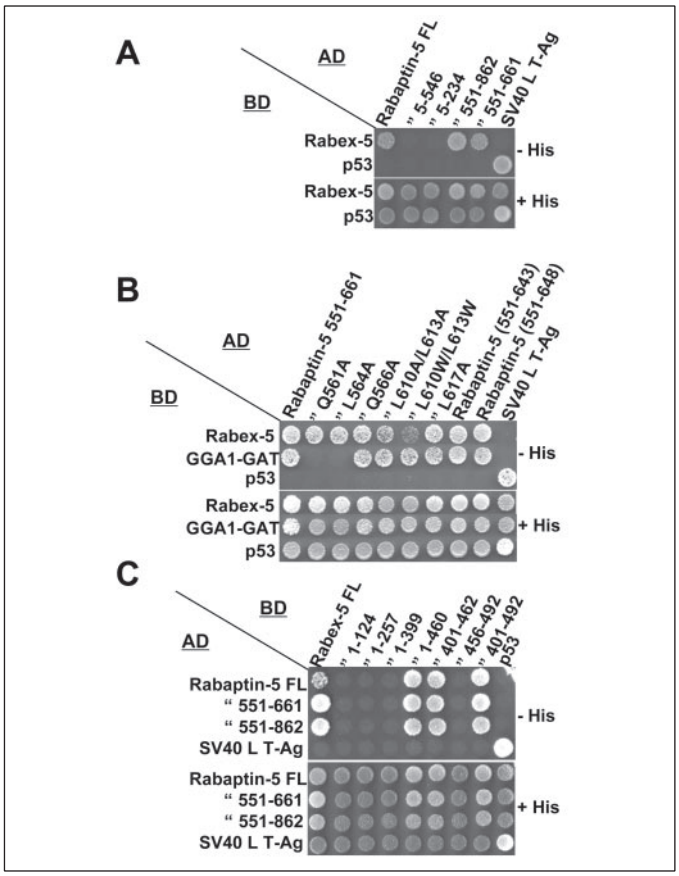

FIGURE 2. **Molecular determinants of the interaction between Rabex-5 and Rabaptin-5.** *A*, yeast two-hybrid analysis showing that Rabex-5 interacts with the Rabaptin-5-(551–661) region. This region in Rabaptin-5 (C2-1 in Fig. 1*B*) also binds the GAT domains of GGA1 and GGA2 (5, 6). The Rabaptin-5 constructs were expressed as Gal4 AD fusions, whereas Rabex-5 was expressed as a Gal4 BD fusion. Yeast co-transformants were plated on medium without histidine (−His) to detect HIS3 reporter gene activation due to interaction of constructs, and on medium with histidine (+His) as a control for loading and growth of the co-transformants. Controls for nonspecific interactions included co-transformation of pGAD constructs with a Gal4 BD-p53 plasmid, as well as co-transformation of pGBT9 constructs with a Gal4 AD-SV40 large T-antigen plasmid (*T-Ag*). Co-transformation with vectors encoding the Gal4 BD-p53 and Gal4 AD-SV40 large T-antigen provided a positive control for interactions. *B*, different binding sites for Rabex-5 and GAT in Rabaptin-5-(551–661). The substitution of residues involved in the stabilization of the Rabaptin-5-(551–661) tetramer (Leu^{610} and Leu^{613}, Ref. 6) decreases the interaction of this construct with Rabex-5. Conversely, the substitution of residues in the GGA1-GAT binding site of Rabaptin-5-(551–661) (such as Gln^{561} or Leu^{564}, Ref. 6) is inconsequential to the binding of Rabex-5. *C*, the Rabex-5-(401–462) region, displaying a high probability of formation of coiled-coils, is both necessary and sufficient for the interaction with either Rabaptin-5 full-length (*FL*) or the Rabaptin-5-(551–661) and -(551–862) fragments. Experiments shown in *B* and *C* were performed as described for *A*.

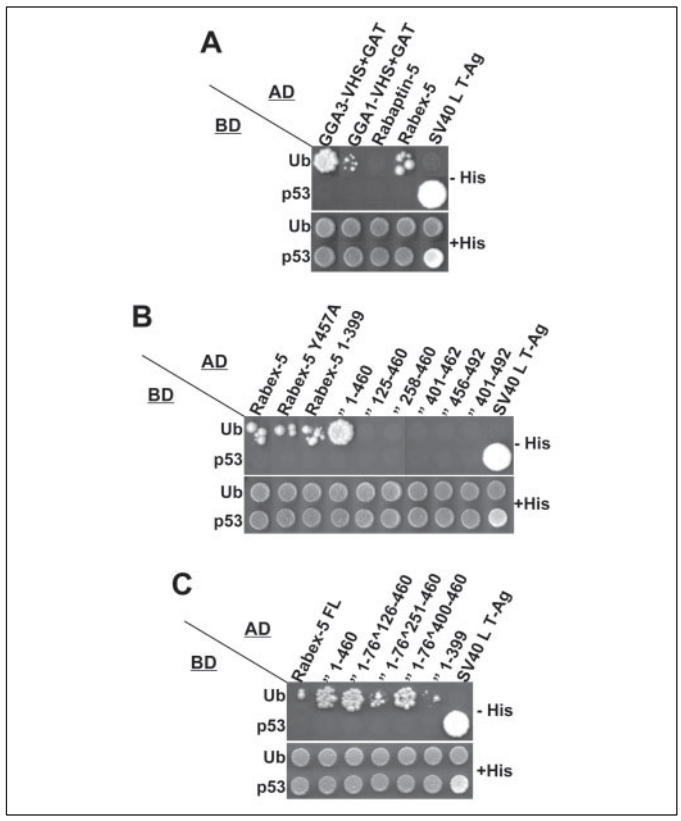

FIGURE 3. **Yeast two-hybrid interaction between Rabex-5 and wild-type ubiquitin.** *A*, Ub interacts with Rabex-5 but not with Rabaptin-5. The constructs for Rabex-5 and Rabaptin-5, as well as the control constructs for GGA3-VHS+GAT and GGA1-VHS+GAT, were expressed as Gal4 AD fusions, whereas Ub was expressed as a Gal4 BD fusion. *B*, substitution of Ala for Rabex-5 Tyr^{457}, a residue proposed to be equivalent to Phe^{420} in the Vps9p C-terminal CUE domain, does not affect the yeast two-hybrid interaction with Ub. The same substitution introduced in a construct displaying a stronger interaction with Ub (Rabex-5-(1–460)) was also inconsequential (results not shown). The Rabex-5-Ub interaction is enhanced by removal of the C-terminal PR region (as shown by the 1–460 fragment) and also by residues in the coiled-coil domain (comparison of 1–399 and 1–460 fragments). *C*, both the N-terminal region (residues 1–76 including the ZnF) and the coiled-coil domain (included in the 400–460 fragment) are important for the interaction between Rabex-5 and wild-type Ub as detected by the yeast two-hybrid system. The Rabex-5 and Ub constructs in *B* and *C* were subcloned in the yeast two-hybrid vectors as described for *A*; experiments were performed as explained in the legend to Fig. 2.

is structurally related to the Ub-associated domain (UBA) (10–12). Substitution of residues in two sequences that are conserved in other CUE domains, MFP and LL corresponding to residues 419–421 and 446–447 in Vps9p, significantly reduced the interaction of this protein with Ub (10–12). Sequence alignment revealed a weak similarity between the Vps9p CUE domain and the corresponding C-terminal region in Rabex-5 where the MFP and LL sequences are replaced by KYP and PL (residues 456–458 and 484–485, respectively) (10). However, replacement of Rabex-5 Tyr^{457}, the residue equivalent to the critical Phe^{420} in Vps9p, had no effect on the yeast two-hybrid interaction with Ub (Fig. 3*B*), suggesting a mode of Ub recognition unrelated to the putative CUE region of Rabex-5. This conclusion was also supported by the lack of interaction between Ub and Rabex-5-(401–492), a construct that contains the region with weak similarity to the Vps9p CUE domain (Fig. 3*B*).

Given that Rabex-5 did not interact with Ub through its putative CUE domain, we prepared a set of Rabex-5 constructs to identify the region involved in this interaction (see Fig. 1*A* for scheme of constructs). The results of the initial analysis showed that the fragments 1–399 and 1–460 exhibited an interaction similar to and significantly higher than, respectively, full-length Rabex-5 in the yeast two-hybrid system (Fig. 3*B*). These results suggested that residues in the coiled-coil region (included in the 1–460 fragment) augmented and in the C-terminal proline-rich domain (included in the full-length construct) diminished the interaction of Rabex-5 with Ub. Additional constructs showed that the Rabex-5 coiled-coil region (construct 401–462) was not sufficient for the interaction with Ub, and that other internal sequences (125–460, 258–460, and 401–492) were also ineffective *per se* (Fig. 3*B*). A possible interpretation of these results is that both the N-terminal (residues 1–124) and the coiled-coil regions of Rabex-5 are necessary for the interaction with Ub detected in the yeast two-hybrid system. This hypothesis was tested by generating and assaying internal deletion constructs (Fig. 3*C*). The results of this analysis showed that a minimal construct containing both the N-terminal 1–76 fragment (including the ZnF domain and residues immediately downstream) and the coiled-coil

region (Rabex-5-(1–76^400–460) in Fig. 3*C*) displayed an interaction with Ub similar to that of Rabex-5-(1–460). Other internal deletion constructs including most of the Vps9 domain or both the HB and the Vps9 domains in addition to the N-terminal 1–76 fragment and the coiled-coil (Rabex-5-(1–76^251–460) and -(1–76^126–460), respectively in Fig. 3*C*) did not display stronger interactions with Ub when compared with the 1–76^400–460 fragment.

Yeast Two-hybrid Analyses Indicate That Rabex-5 Interactions with Ubiquitin Involve Both Non-covalent Binding and Covalent Modification—It has been recently reported that one of the ZnF domains present in the C-terminal region of A20, an inhibitor of tumor necrosis factor (TNF) receptor signaling, displays Ub ligase (E3) activity and catalyzes Lys^{48}-linked polyubiquitination (23). This observation led us to question whether the interaction between Rabex-5 and Ub detected with the two-hybrid system reflected a binding event or, alternatively, the covalent ubiquitination of Rabex-5 on one or more lysine residues catalyzed by its own ZnF. We analyzed this possibility using an Ub mutant (ΔG75/G76) that is unable to undergo covalent attachment through the formation of an isopeptide bond between its C-terminal glycine and the ϵ-amino group of lysines in the target proteins. Yeast two-hybrid analyses (Fig. 4*A*) showed that Rabex-5-(1–399) and -(1–460) exhibit weak binding to UbΔG75/G76 and that most of the interaction detected between these constructs and wild-type Ub represents covalent attachment. The experiments with UbΔG75/G76 and Rabex-5-(456–492) confirmed that the putative CUE region of Rabex-5 does not bind Ub. The weak binding signals observed with ΔG75/G76 Ub and Rabex-5-(1–399) and -(1–460) in our yeast two-hybrid assay using Gal4 BD and AD vectors can be explained by the relatively low affinity binding of Ub to its various binding domains (24–25). We also observed strong and weak signals with wild type and ΔG75/G76 Ub, respectively, when studying the yeast two-hybrid interaction of these constructs with GGA3, another protein that both binds Ub and undergoes ubiquitination (22) (results not shown).

A final aspect analyzed using the yeast two-hybrid system was whether the ubiquitination of Rabex-5 was dependent on the structure of its ZnF. To this end, we substituted the four conserved Cys residues that are present in the Rabex-5 ZnF in the context of the Rabex-5-(1–76^400–460) construct. A similar substitution of conserved Cys residues in the fourth Cys_2/Cys_2 ZnF domain of A20 markedly reduced the Lys^{48}-linked polyubiquitination of the TNF receptor 1-interacting protein (23). Whereas the simultaneous substitution of two Cys residues in the Rabex-5 ZnF (either C19A/C23A or C35A/C38A) had little effect, the combined substitution of all four residues (C19A/C23A/C35A/C38A) significantly reduced, but did not completely abolish, the interaction with Ub in the yeast two-hybrid system (Fig. 4*B*). In summary, the results using the yeast two-hybrid system were consistent with the notion that Rabex-5 both binds and undergoes covalent attachment of Ub, and that the ubiquitination of this protein is partially dependent on the structure of its N-terminal ZnF.

Pull-down Assays Reveal That the Rabex-5 Atypical UIM Binds Ubiquitin—The yeast two-hybrid analysis using ΔG75/G76 Ub and the Rabex-5-(1–399) and -(1–460) fragments suggested the presence of a "true" Ub-binding site in Rabex-5 (Fig. 4*A*). Analysis of the sequence downstream from the Rabex-5 ZnF (α1 in Fig. 1*A*) revealed a stretch (WELAERLQREE; residues 55–65) that matched, with the exception of a Gln for Ser substitution, the core region of the consensus Ub-interacting motif (UIM) (Φ*XX*A*XXX*S*XX*Ac, where Φ represents an hydrophobic residue, *X* denotes any amino acid, and Ac an acidic residue) (26). The WELAERLQREE sequence in Rabex-5 is also preceded by acidic residues (Glu^{53} and Asp^{54}) as in the consensus UIM (26). To test

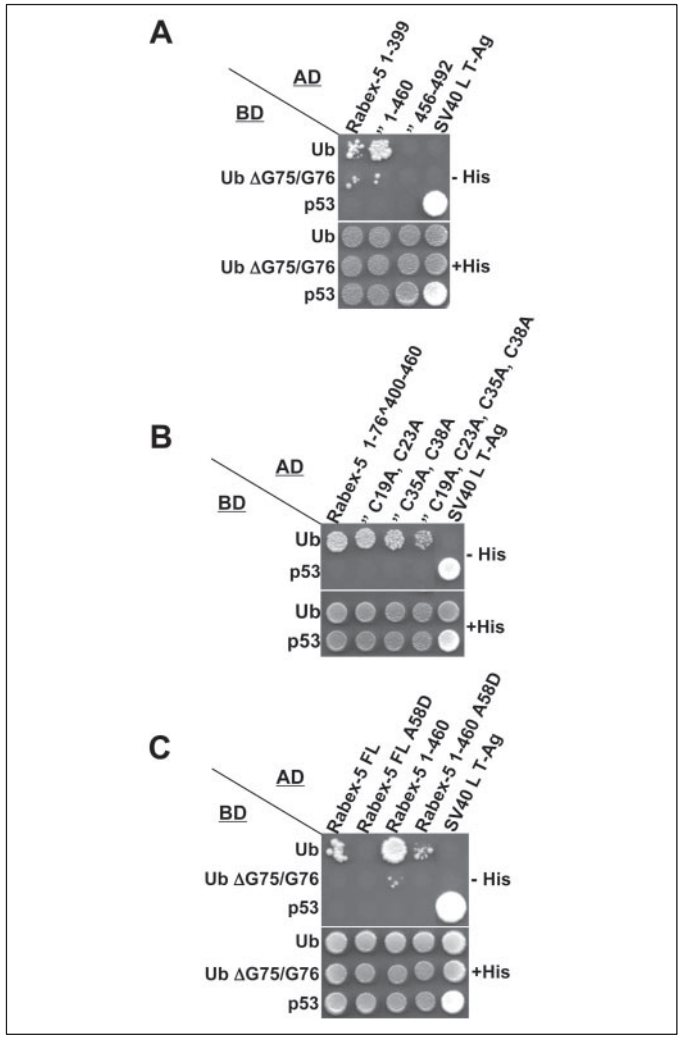

FIGURE 4. **Distinction of noncovalent binding and covalent attachment of Ub to Rabex-5 using the yeast two-hybrid system; role of the Cys_2/Cys_2 ZnF and Ala^{58} in the Rabex-5-Ub interaction.** *A*, experiments with ΔG75/G76 Ub show that most of the yeast two-hybrid interactions detected between wild-type Ub and Rabex-5-(1–399) or Rabex-5-(1–460) represent covalent ubiquitination of these constructs. The Rabex-5 PR domain (residues 456–492, including the Tyr^{457} in the putative CUE motif) does not bind ΔG75/G76 Ub. *B*, simultaneous substitution of all four Cys, but not of two such residues, in the Cys_2/Cys_2 ZnF reduces the interaction of Rabex-5 with wild-type Ub. *C*, Rabex-5 Ala^{58} is required for both Ub binding (see also Fig. 5*B*) and covalent attachment of Ub, as shown by the decrease in the interactions of wild-type Ub with Rabex-5 full length (*FL*) and the 1–460 fragment. Constructs were subcloned in the yeast two-hybrid vectors as explained in the legend to Fig. 3*A*; experiments were performed as described in the legend to Fig. 2.

whether this sequence could indeed bind Ub we generated two GST fusions, one comprising the ZnF but excluding the WELAERLQREE sequence (GST-Rabex-5-(1–49)) and the other including both the ZnF and the putative Ub binding site (GST-Rabex-5-(1–76)) and tested their ability to bind non-covalently to Ub-agarose beads. GST-β3B ear and GST-GGA1-VHS+GAT were used as negative and positive controls, respectively, for binding to Ub-agarose (13) and protein A-agarose as control for nonspecific binding. The results in Fig. 5*A* show that Rabex-5-(1–76) binds to Ub-agarose with high avidity, but not to the protein A-agarose control; on the other hand, the Rabex-5-(1–49) construct excluding the WELAERLQREE sequence exhibited markedly reduced binding to Ub-agarose compared with Rabex-5-(1–76). Nonetheless, the Rabex-5-(1–49) construct displayed some residual binding, suggesting that the ZnF may also contribute to the overall interaction. We also addressed whether the WELAERLQREE box in Rabex-5-(1–76)

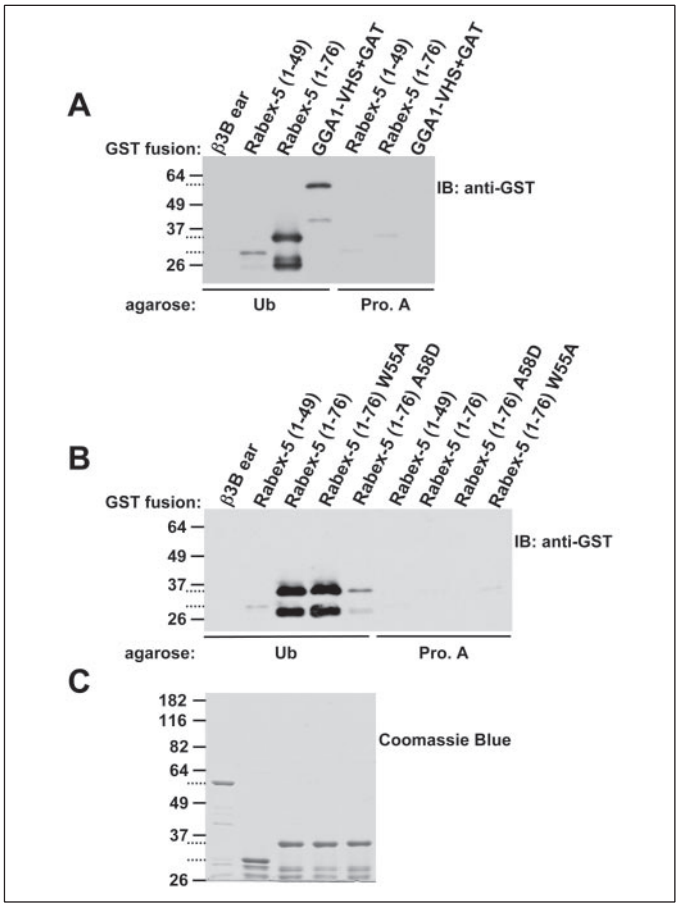

FIGURE 5. **In vitro binding of Rabex-5 to Ub.** *A*, the indicated GST fusions were incubated with Ub-agarose or protein A-agarose; the proteins bound to the washed beads were eluted and subjected to SDS-PAGE and immunoblotting with anti-GST antiserum. The experiments included GST-β3B ear and GST-GGA1-VHS+GAT as negative and positive controls, respectively. *B*, the A58D substitution impairs the binding of GST-Rabex-5-(1–76) to Ub-agarose. The experiments were performed as described for *A*. *Dotted lines* at the *left* of the panels indicate the position of full-length constructs; faster migrating species probably correspond to degradation products or truncated proteins. *C*, Coomassie Blue staining of the GST fusions used in the experiments depicted in *A* and *B* (order of samples is as labeled in *B*). Numbers at the *left* of each panel indicate the positions of molecular mass markers (in kDa).

was responsible for the binding to Ub-agarose by testing the effect of the W55A and A58D substitutions in this sequence. Whereas the former (W55A) was inconsequential, the latter (A58D) caused a marked reduction in binding to Ub-agarose (Fig. 5*B*). The importance of the Rabex-5 Ala^{58} residue in the binding of Ub is consistent with the role played by the equivalent Ala residues in the UIM of Hrs and Vps27p (25, 27) and S5a (28). These experiments demonstrated that an atypical UIM and, to a lesser extent, the adjacent ZnF in Rabex-5-(1–76) mediate non-covalent binding to Ub in this *in vitro* system.

The Rabex-5 ZnF Has Ubiquitin Ligase Activity in Vitro—Our yeast two-hybrid analysis and the reported Ub ligase (E3) activity of one of the ZnF domains of A20 (23) prompted the question of whether the cognate domain of Rabex-5 displays a similar activity. This was analyzed by *in vitro* ubiquitination experiments using bacterially expressed GST fusions encompassing only the Rabex-5 ZnF, or this domain plus the downstream regions implicated in Ub binding (GST-Rabex-5-(1–49) and GST-Rabex-5-(1–76), respectively). Unlike the GST control, GST-Rabex-5-(1–76) displayed significant E3 activity and catalyzed ubiquitination in the presence of Ub-conjugating enzymes (Ubc) (particularly UbcH5A and UbcH5C), but not in their absence (Fig. 6*A*). Although this *in vitro* ubiquitination assay can measure both E3 autoubiquitination and the formation of free poly(Ub) chains, the lower limit of the range of strong anti-Ub immunoreactivity (~45 kDa) suggests the possible autoubiquitination of GST-Rabex-5-(1–76) (Fig. 6*A*). The preference of GST-Rabex-5-(1–76) for UbcH5A and UbcH5C contrasted with that of the control GST-X-linked inhibitor of apoptosis (XIAP), which exhibited E3 activity in the presence of UbcH5B and UbcH7 (Fig. 6*B*). The selectivity of the GST-Rabex-5-(1–76) for UbcH5A and UbcH5C was not caused by a higher activity of these E2 enzymes as demonstrated by the control thiolester assays shown in Fig. 6*C*. Finally, similar E3 activities were observed when assaying the GST-Rabex-5-(1–49), -(1–76), or -(1–76) A58D constructs in the presence of UbcH5C (Fig. 6*D*). This result indicates that the E3 activity measured *in vitro* with exogenously added E2 is intrinsic to the Rabex-5 ZnF and does not require the contiguous UIM variant.

Rabex-5 Is Ubiquitinated in HeLa Cells—We tested the hypothesis that Rabex-5 undergoes ubiquitination *in vivo* by performing experiments with HeLa cells transiently co-transfected with vectors directing the expression of $(HA)_3$-Ub and either Myc-Rabex-5 or Myc-stonin 2 proline-rich (PR) domain (epitope tags were placed at the N terminus of all proteins). Immunoprecipitation of the transfected cell extracts with anti-Myc antibodies showed significant ubiquitination of Myc-Rabex-5 but not of the Myc-stonin 2-PR domain used as control (Fig. 7*A*, *left blot*). The stoichiometry of ubiquitination of Rabex-5 was estimated by comparing the apparent molecular masses of ubiquitinated-Myc-Rabex-5 (monoclonal anti-HA immunoblots) and Myc-Rabex-5 (monoclonal anti-Rabex-5 immunoblots). The anti-HA immunoblots showed a band at ~80 kDa (Fig. 7*A*, *left blot*); those obtained with anti-Rabex-5 displayed a main band at ~64 kDa, accompanied by two relatively weak upper bands in the 70–80 kDa range and a weak lower band at ~57 kDa that were visible after more prolonged exposures (Fig. 7*A*, *center blot*). The upper band detected with anti-Rabex-5 (representing ~5–10% of the total Rabex-5 signal) coincided with the band corresponding to ubiquitinated-Rabex-5 as detected with anti-HA (Fig. 7*A*). Furthermore, the difference in apparent molecular masses (~80 kDa for HA-ubiquitinated Myc-Rabex-5 and ~64 kDa for the main band of Myc-Rabex-5) was similar to the predicted mass of the $(HA)_3$-Ub construct (12.5 kDa). This analysis suggests that ~5–10% of the recombinant Rabex-5 undergoes monoubiquitination in HeLa cells. The second band from the top detected with anti-Rabex-5 may represent another covalent modification of Rabex-5 or a degradation product of the monoubiquitinated Rabex-5 (we cannot rule out that the top band seen with anti-Rabex-5 may also include another form of Myc-Rabex-5 coinciding in mobility with HA-monoubiquitinated-Myc-Rabex-5). An alternative interpretation is that the two upper bands detected with anti-Rabex-5 may represent mono- and di-ubiquitinated forms of Rabex-5 (in order of increasing molecular mass). We believe that this interpretation is less likely considering that we observed a single clear band corresponding to ubiquitinated Rabex-5 in the anti-HA immunoblots, as opposed to two bands corresponding to the covalent attachment of one and two Ub moieties. However, the possibility of diubiquitination, or of monoubiquitination in two different acceptor lysines, cannot be completely ruled out given possible errors in the assignment of the apparent molecular masses. The anti-Myc immunoprecipitates were also immunoblotted with anti-Myc. This analysis revealed two bands with identical apparent molecular mass but reciprocal intensities when compared with the ~64- and 57-kDa bands detected with anti-Rabex-5 representing full-length and cleaved Myc-Rabex-5, respectively (Fig. 7*A*, *center* and *right blots*). Given the ~7 kDa difference in mass between these bands and that the monoclonal anti-Rabex-5 recognizes a C-terminal epitope (residues 426–456, "Experimental Procedures"), the change in the relative

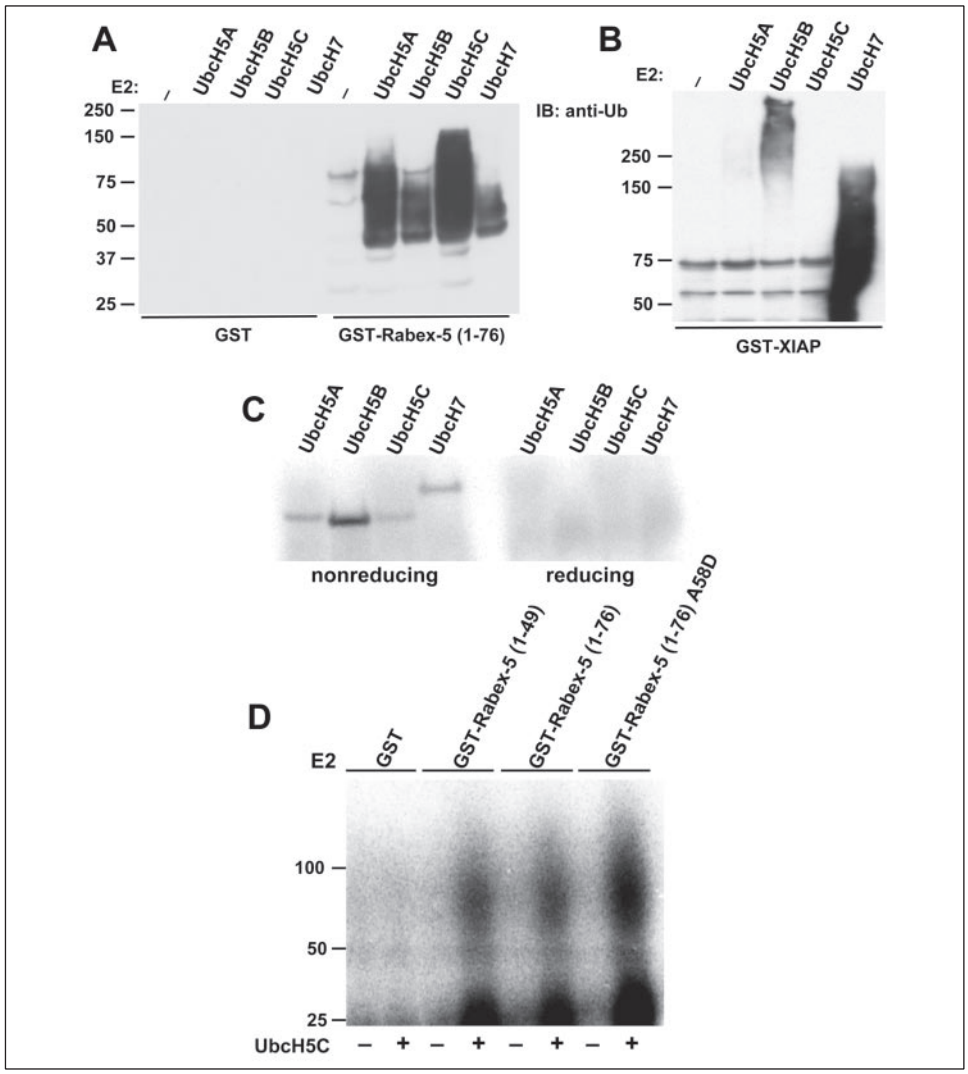

FIGURE 6. **E3 activity of the Rabex-5 zinc finger.** *A* and *B*, the Ub ligase (E3) activity of GST-Rabex-5-(1–76) was assayed *in vitro* in the presence or absence of the indicated Ub-conjugating (Ubc) enzymes (E2). GST and GST-XIAP were used as negative and positive controls, respectively. The incubations were performed in the presence of 10 μM ubiquitin, and the samples were subsequently subjected to immunoblotting with rabbit polyclonal anti-Ub. *C*, thiolester formation assay for the different E2 enzymes used in *A* and *B*. Following incubation in the presence of ^{32}P-labeled-Ub, the samples were resuspended in nonreducing or reducing sample buffer and subjected to SDS-PAGE followed by phosphor screen imaging. *D*, the GST-Rabex-5-(1–49), -(1–76), and -(1–76) A58D constructs display similar E3 activities. The reaction mixtures contained 0.02 μCi of ^{32}P-labeled Ub, and the samples were subsequently subjected to SDS-PAGE and phosphor screen imaging. Numbers on the *left* of each panel indicate the positions of molecular mass markers (in kDa).

intensities of these bands when blotted with anti-Rabex-5 or anti-Myc is likely caused by a marked decrease in the affinity of the monoclonal anti-Rabex-5 for a Rabex-5 fragment cleaved in the 426–456 region (~57-kDa band in Fig. 7*A*, *center* and *right blots*).

The ubiquitination of Myc-Rabex-5 could result from the expression of relatively high levels of this recombinant protein in HeLa cells. Consequently, we analyzed the possible ubiquitination of endogenous Rabex-5 in HeLa cells, and also the ubiquitination status of the Rabex-5 that is part of a functionally relevant complex with Rabaptin-5. To this end, extracts of HeLa cells transfected with $(HA)_3$-Ub were immunoprecipitated with either anti-Rabex-5 or anti-Rabaptin-5 antisera followed by SDS-PAGE and immunoblotting. The results obtained (Fig. 7*B*) showed that both the total endogenous Rabex-5 as well as the endogenous Rabex-5 co-immunoprecipitated by anti-Rabaptin-5 undergo ubiquitination, consistent with the idea that this modification may have functional relevance. A comparative analysis of molecular masses similar to that performed for Myc-Rabex-5 indicates that the endogenous Rabex-5 also appears to undergo monoubiquitination.

The binding of Ub to some CUE- or UIM-containing proteins is required for their monoubiquitination at sites outside their CUE or UIM domains, which is catalyzed by separate Ub ligases (8, 9, 29). Given that Rabex-5 binds Ub (Fig. 5), undergoes ubiquitination (Fig. 4*A* and Fig. 7, *A* and *B*) and displays Ub ligase activity (Fig. 6), we asked whether the ubiquitination of Rabex-5 was dependent on either the presence of its ZnF or on the integrity of the downstream Ub binding site. We observed that the deletion of the ZnF and the A58D substitution markedly reduced and completely abrogated, respectively, the ubiquitination of Rabex-5 (Fig. 7*C*, *left blot*). The reduction in ubiquitination was observed despite the fact that the expression of both mutants was higher than that of wild-type Myc-Rabex-5 (Fig. 7*C*, *right blot*). These results demonstrate that whereas the recruitment of additional E3 enzymes may partially complement the activity of the ZnF, the binding of Ub to the sequence around Ala^{58} appears essential for the ubiquitination of Rabex-5 in HeLa cells. The relationship between binding and covalent attachment of Ub to Rabex-5 was also analyzed with the yeast two-hybrid system using wild-type Ub (to evaluate mainly ubiquitination) and ΔG75/G76 Ub (to assess Ub binding). Consistent with the observations in transfected HeLa cells, the A58D substitution introduced in the full-length or the 1–460 fragment of Rabex-5 eliminated and markedly reduced, respectively, the interaction of these constructs with wild-type Ub in the two-hybrid system (Fig. 4*C*). The A58D substitution also impaired the weak binding of Rabex-5-(1–460) to ΔG75/G76 Ub (Fig. 4*C*), in agreement with the effect of this substitution on the *in vitro* binding of GST-Rabex-5-(1–76) to Ub (Fig. 5*B*). Taken together, these experiments demonstrate the ubiquitination of Rabex-5 and the importance of the ZnF and downstream Ub binding sequence in this covalent modification.

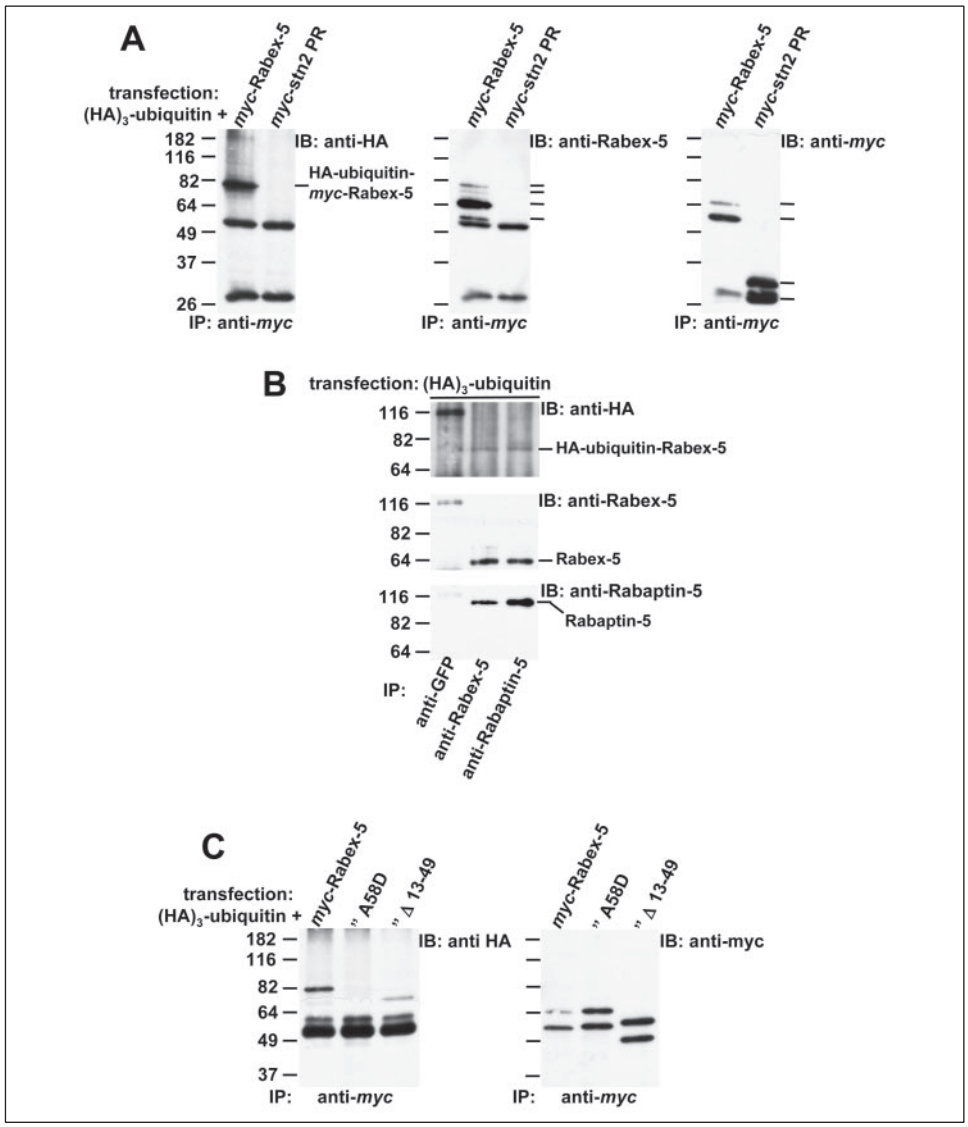

FIGURE 7. **Ubiquitination of Rabex-5 in HeLa cells.** *A*, HeLa cells were co-transfected with $(HA)_3$-Ub and either Myc-Rabex-5 or Myc-stonin 2 proline-rich domain (*Myc-stn2 PR*). All epitope tags were located at the N termini of the recombinant proteins. At 12–16 h post-transfection, cells were lysed and subjected to immunoprecipitation with mouse monoclonal anti-Myc**.** The immunoprecipitates were subjected to SDS-PAGE and immunoblotting with mouse monoclonal anti-HA (*blot at left*), mouse monoclonal anti-Rabex-5 (*center blot*), or a polyclonal antiserum to Myc (*blot at right*). The position of immunoprecipitated proteins is shown with *lines* at the *right side* of each panel. *B*, HeLa cells transfected with $(HA)_3$-Ub were subjected to immunoprecipitation with either mouse monoclonal anti-GFP, rabbit polyclonal antiserum to Rabex-5, or goat polyclonal antiserum to Rabaptin-5, as indicated at the *bottom* of the panel. The immunoprecipitated samples were subsequently subjected to SDS-PAGE and immunoblotting with mouse monoclonal anti-HA (*top blot*), mouse monoclonal anti-Rabex-5 (*center blot*), or mouse monoclonal anti-Rabaptin-5 (*bottom blot*). The ~116-kDa band visualized in the *first lane at left* with anti-HA, and to a lower extent with anti-Rabex-5 and anti-Rabaptin-5, represents an unrelated protein immunoprecipitated by the control anti-GFP. (This antibody did not immunoprecipitate Rabex-5 or Rabaptin-5.) *C*, HeLa cells were co-transfected with $(HA)_3$-Ub and either Myc-Rabex-5, Myc-Rabex-5 A58D, or a Myc-Rabex-5 construct lacking its ZnF (Myc-Rabex-5Δ13–49). Cell lysates were subjected to immunoprecipitation with mouse monoclonal anti-Myc followed by SDS-PAGE and immunoblotting with mouse monoclonal anti-HA or rabbit polyclonal anti-Myc. The immunoblotting images shown in each panel were obtained by successive blotting and stripping cycles of a single transferred membrane. Numbers at the *left* of each panel indicate the positions of molecular mass markers (in kDa).

DISCUSSION

This study represents the first demonstration that Rabex-5 is an Ub ligase that binds Ub and undergoes ubiquitination. This study also identifies residues that are critical for the binding and covalent attachment of Ub and defines the molecular determinants responsible for the interaction of Rabex-5 with Rabaptin-5.

Structural Determinants for the Interaction of Rabex-5 with Rabaptin-5—The definition of the domains involved in the interaction between Rabex-5 and Rabaptin-5 explains how they form multimeric complexes with themselves and other proteins. Our experiments show that the molecular determinants of this interaction reside in the Rabaptin-5 C2–1 coiled-coil (residues 551–661) and in the Rabex-5 coiled-coil (residues 401–462) (Fig. 2). Of interest, the residues in the Rabaptin-5 C2–1 coiled-coil that are critical to the interaction with the GGA1-GAT domain (6) do not participate in the interaction with Rabex-5 (Fig. 2*B*). The identification of the domains involved in the Rabex-5-Rabaptin-5 interaction (Fig. 2, *A–C*), along with the other structural features of these molecules summarized in Fig. 1, indicate that the Rabex-5·Rabaptin-5 complex can simultaneously interact with GGAs, Rab4, and Rab5, given that their corresponding binding sites are not mutually exclusive. A possible variation in the assembly of multimeric complexes including Rabex-5 and Rabaptin-5 is suggested by the demonstration that substitution of residues involved in the stabilization of Rabaptin-5-(551–661) tetramers (6) also interferes with the binding to Rabex-5 (Fig. 2*B*). This observation suggests that the binding of Rabex-5 could affect the oligomerization of Rabaptin-5. At the same time, the identification of the Rabex-5 coiled-coil as the region that binds Rabaptin-5 (Fig. 2*C*) represents an important first step in the mapping of the domains that sense regulatory signals responsible for increasing the low intrinsic Rab5 GEF activity of full-length Rabex-5 (2, 3). In this context, Delprato *et al.* (3) showed that the isolated HB-Vps9 tandem domains of Rabex-5 (residues 132–391) have a much higher GEF activity on Rab5 than the full-length protein. The observations in the present study suggest that the interaction of the Rabex-5 coiled-coil with Rabaptin-5 might relieve the inhibition of the Rabex-5 HB-Vps9 GEF activity exerted by sequences located N- and/or C-terminal to this tandem.

Rabex-5 Binds Ubiquitin—A second aspect of the Rabex-5 interactions revealed by this study is the demonstration that this molecule binds Ub. Importantly, Ub does not bind to the C-terminal region of Rabex-5 that was predicted to contain a sequence with low similarity to the Vps9p CUE domain (10). Rather, we demonstrate the presence of a

Ub binding site in an α-helical region located immediately C-terminal to the ZnF domain (Fig. 5). This segment comprises the sequence WELAERLQREE (residues 55–65 of Rabex-5), which conforms to the core region of the consensus Ub-interacting motif (UIM) Φ*XX*A*XXX*-S*XX*Ac (Φ, position 0 of the core motif, represents an hydrophobic residue, *X* denotes any residue and Ac an acidic residue), with the exception of the presence of Gln^{62} in place of a Ser at +7 (26). The role of this putative UIM in the interaction with Ub is supported by the impairment caused by substitution of Asp for Ala^{58} in the context of the Rabex-5-(1–76) fragment (Fig. 5*B*). The substitution of Gln^{62} for the Ser present in the consensus UIM does not seem to preclude Ub binding (Fig. 5, *A* and *B*), a finding that is consistent with the modest (~2-fold) decrease in affinity for Ub caused by the mutation of Ala for Ser at +7 in the Hrs UIM (25). The modest effects of substituting Gln or Ala for the Ser at +7 in the core UIM are in contrast with the marked reduction in Ub binding caused by the less conservative mutations to Asp or Glu at this position in the UIMs of Vps27p (30) and Hrs (24), and also with the significant effects of substituting the Ala at +3 in both the Rabex-5-(1–76) (Fig. 5*B*) and Hrs motifs (25). A search of data bases for Rabex-5 orthologs showed that the basic architecture of this atypical core UIM (Trp at 0, Ala at +3, Gln at +7, and Glu at +10) has been conserved in vertebrates, but not in insects or nematodes (data not shown). Whereas the binding and the covalent attachment of Ub to Rabex-5 complicated the initial interpretation of the yeast two-hybrid assays carried out with wild-type Ub, the simultaneous use of wild-type and ΔG75/76 Ub (Fig. 4) allowed the dissection of these two events. These experiments underscore the importance of using the ΔG75/G76 Ub mutant to identify Ub-binding proteins in yeast two-hybrid screens. Such an approach, using LexA BD-Ub ΔG75/76 as bait and a VP16 trans-AD library, allowed the identification of the Vps9p Cue1p-homologous (CUE) domain as an Ub binding module (10).

E3 Activity of the Rabex-5 ZnF—The demonstration that the Rabex-5 ZnF domain displays Ub ligase (E3) activity represents a third important observation in this study (Fig. 6). E3 enzymes specify the timing and substrate selection and are the key regulators of ubiquitination reactions (7). The presence of separate domains displaying binding of Ub and E3 activity endow Rabex-5 with the potential of regulating its own ubiquitination through the interaction with other Ub-binding proteins and/or of acting as an E3 for other Ub-binding proteins. Whereas the structures of the ZnF in Rabex-5 and in RING type- and PHD domain-containing E3 enzymes are different, the Rabex-5 ZnF is related to a cognate domain in the protein A20 which displays E3 activity (23). A20 inhibits NF-κB signaling by increasing the degradation of receptor-interacting protein (RIP), an essential effector of the tumor necrosis factor receptor 1. The increased degradation of RIP triggered by A20 results from two intrinsic activities of this molecule: the de-ubiquitinating activity of its N-terminal domain, which removes Lys^{63}-linked Ub chains (and also Lys^{48} chains), and the E3 activity of one of its C-terminal ZnF, which catalyzes Lys^{48}-linked polyubiquitination leading to increased proteasomal degradation of RIP (23, 31). A20 contains seven ZnF that conform to the general pattern $CX_{2-4}C_{11}CXXC$ (32) and can be further clustered in two subgroups: ZnF 1, 2, 3, 5–7, and ZnF 4, respectively (23). In the alignment reported by Wertz *et al.* (23), the Rabex-5 ZnF, which displays E3 activity (Fig. 6), specifically clusters with the A20 ZnF 4, which is responsible for the E3 activity of A20. These findings are consistent with the prediction that Cys_2/Cys_2 ZnF containing an acidic residue in the third position distal to the last cysteine (Glu^{41} in Rabex-5) may represent a novel family of E3 enzymes. However, the predicted presence of a large residue in the eight position distal to the last cysteine (23) does not seem indispensable, because this position corresponds to Ala^{46} in Rabex-5.

In Vivo Ubiquitination of Rabex-5—The observations shown in Fig. 7 demonstrate the *in vivo* ubiquitination of Rabex-5. Importantly, we demonstrate the ubiquitination of endogenous Rabex-5 that is part of a functionally relevant complex with Rabaptin-5 (Fig. 7*B*). The covalent attachment of Ub to Rabex-5, which depends to a significant extent on the presence of its ZnF, did not appear to result in formation of poly(Ub) chains (Fig. 7). This contrasts with the polyubiquitination catalyzed by the A20 ZnF (23). It is possible that this difference reflects the intrinsic E3 catalytic properties of these two ZnF or, alternatively, that the binding of the Rabex-5 UIM to covalently attached Ub prevents subsequent chain formation. It should be noted that Rsp5/Nedd4 and Cbl E3s can promote either mono- or polyubiquitination, and that the final reaction product may depend on the presence of regulatory proteins that control the temporal association of E3 enzymes with their substrates (7, 9). As mentioned, the deletion of the ZnF domain markedly reduces, although does not completely abolish, the ubiquitination of Rabex-5 (Fig. 7*C*). This indicates that whereas the intrinsic E3 activity of its ZnF leads to the ubiquitination of Rabex-5, other Ub ligases may contribute to it. This interpretation is also consistent with the partial effects seen in the yeast two-hybrid assays following substitution of the Rabex-5 ZnF Cys residues (Fig. 4*B*). Previous studies reported that Vps9p ubiquitination is dependent on both a functional CUE domain and Rsp5p, a yeast HECT domain E3 enzyme of the Nedd4 family (33), and that Nedd4 can ubiquitinate eps15 in a UIM-dependent manner (34). These observations suggested the notion that CUE and UIM domains in these proteins may recognize Ub-HECT E3 thiolester intermediates leading to subsequent ubiquination of residues outside the CUE and UIM domains (7, 34). It is important to note that the ubiquitination of Rabex-5 also requires the presence of a functional Ub-binding site (experiments with Rabex-5 A58D shown in Fig. 7*C*). We speculate that the internal UIM may be necessary to recruit Ub-E2 complexes and/or Ub-heterologous E3 complexes that may also contribute to the ubiquitination of Rabex-5. It is also noteworthy that whereas both the ZnF and an intact UIM domain are important for ubiquitination of Rabex-5 in HeLa cells (Fig. 7*C*), the *in vitro* E3 activity is only dependent on its ZnF (Fig. 6*D*). We postulate that only the Rabex-5 Zn finger is required for E3 *in vitro* activity because of the high concentrations of exogenously added E2 and Ub used in this assay. The more stringent requirement for the *in vivo* ubiquitination may reflect the need to enhance activity under conditions where components of the ubiquitination machinery are more limiting and subjected to spatial and temporal regulation.

Possible Role of Ubiquitin-dependent Modifications in Rabex-5 Function—The mono- or diubiquitination of specific substrates (such as transmembrane receptors, transporters, or channels) acts as a signal for their internalization, endosomal targeting or sorting at the TGN (7, 9). The transduction of the ubiquitination transport signal is carried out by a complex set of proteins that either bind Ub or undergo ubiquitination and, in some instances, are endowed with both properties. Steps regulated by specific transducers of ubiquitinated signals include the sorting of ubiquitinated receptors at the plasma membrane (involving proteins such as epsins, Eps15, CIN85, Numb, β-arrestin, and Comm) and endosomes (involving Hrs/Vps27, STAM/Hse1, and the ESCRT-I, -II, and -III complexes, Refs. 7 and 9). It has been recently demonstrated that Vps9p (the yeast ortholog of Rabex-5) binds to Ub and undergoes ubiquitination, and that the deletion of its CUE domain rescues endosomal trafficking defects of receptors lacking Ub signals (8, 10, 33). This suggested an autoregulatory cycle whereby the Vps9p CUE domain may bind to the Ub moiety that is covalently attached to a separate region of

this protein to yield a GEF inactive form. Under this hypothesis, the competition for the Vps9p CUE by other ubiquitinated proteins might result in a conformational change and activation of Vps9p, leading to trafficking of ubiquitinated cargo to different intracellular compartments (8, 10). The precise role of Rabex-5 ubiquitination in the coordination of one or more intracellular transport steps and the identity of the ubiquitinated cargo and Ub-binding proteins specifically interacting with Rabex-5 remain to be elucidated. The possible concerted regulation of Rabex-5 activity through its ubiquitination and binding of ubiquitinated proteins and Rabaptin-5 is another aspect that deserves further study.

Acknowledgments—We thank J. Hurley and S. Lee for critical reading of the manuscript, and H. Tsai and X. Zhu for expert technical assistance. We are also indebted to M. Zerial for his generous gift of anti-Rabex-5 antiserum and pGEMT-Rabex-5 construct.

REFERENCES

1. Horiuchi, H., Lippé, R., McBride, H. M., Rubino, M., Woodman, P., Stenmark, H., Rybin, V., Wilm, M., Ashman, K., Mann, M., and Zerial, M. (1997) *Cell* **90,** 1149–1159
2. Lippé, R., Miaczynska, M., Rybin, V., Runge, A., and Zerial, M. (2001) *Mol. Biol. Cell* **12,** 2219–2228
3. Delprato, A., Merithew, E., and Lambright, D. G. (2004) *Cell* **118,** 607–617
4. Vitale, G., Rybin, V., Christoforidis, S., Thornqvist, P., McCaffrey, M., Stenmark, H., and Zerial, M. (1998) *EMBO J.*, **17,** 1941–1951
5. Mattera, R., Arighi, C. N., Lodge, R., Zerial, M., and Bonifacino, J. S. (2003) *EMBO J.* **22,** 78–88
6. Zhu, G., Zhai, P., He, X., Wakeham, N., Rodgers, K., Li, G., Tang, J., and Zhang, X. C. (2004) *EMBO J.* **23,** 3909–3917
7. Hicke, L., and Dunn, R. (2003) *Annu. Rev. Cell Dev. Biol.* **19,** 141–172
8. Di Fiore, P. P., Polo, S., and Hofmann, K. (2003) *Nat. Rev. Mol. Cell. Biol.* **4,** 491–497
9. Haglund, K., Di Fiore, P. P., and Dikic, I. (2003) *Trends Biochem. Sci.* **28,** 598–603
10. Donaldson, K. M., Yin, H., Gekakis, N., Supek, F., and Joazeiro, C. A. (2003) *Curr. Biol.* **13,** 258–262
11. Shih, S. C., Prag, G., Francis, S. A., Sutanto, M. A., Hurley, J. H., and Hicke, L. (2003) *EMBO J.* **22,** 1273–1281
12. Prag G., Misra, S., Jones, E. A., Ghirlando, R., Davies, B. A., Horazdovsky, B. F., and Hurley, J. H. (2003) *Cell* **113,** 609–620
13. Mattera, R., Puertollano, R., Smith, W. J., and Bonifacino, J. S. (2004) *J. Biol. Chem.* **279,** 31409–31418
14. Puertollano, R., and Bonifacino, J. S. (2004) *Nat. Cell. Biol.* **6,** 244–251
15. Sheffield, P., Garrard, S., and Derewenda, Z. (1999) *Protein Expr. Purif.* **15,** 34–39
16. Yang, Y., Fang, S., Jensen, J. P., Weissman, A. M., and Ashwell, J. D. (2000) *Science* **288,** 874–877
17. Martina, J. A., Bonangelino, C. J., Aguilar, R. C., and Bonifacino, J. S. (2001) *J. Cell. Biol.* **153,** 1111–1120
18. Dell'Angelica, E. C., Klumperman, J., Stoorvogel, W., and Bonifacino, J. S. (1998) *Science* **280,** 431–434
19. Cenciarelli, C., Wilhelm, K. G., Jr., Guo, A., and Weissman, A. M. (1996) *J. Biol. Chem.* **271,** 8709–8713
20. Scheffner, M., Huibregtse, J. M., and Howley, P. M. (1994) *Proc. Natl. Acad. Sci. U. S. A.* **91,** 8797–8801
21. Jensen, J. P., Bates, P. W., Yang, M., Vierstra, R. D., and Weissman, A. M. (1995) *J. Biol. Chem.* **270,** 30408–30414
22. Shiba, Y., Katoh, Y., Shiba, T., Yoshino, K., Takatsu, H., Kobayashi, H., Shin, H. W., Wakatsuki, S., and Nakayama, K. (2004) *J. Biol. Chem.* **279,** 7105–7111
23. Wertz, I. E., O'Rourke, K. M., Zhou, H., Eby, M., Aravind, L., Seshagiri, S., Wu, P., Wiesmann, C., Baker, R., Boone, D. L., Ma, A., Koonin, E. V., and Dixit, V. M. (2004) *Nature* **430,** 694–699
24. Raiborg, C., Bache, K. G., Gillooly, D. J., Madshus, I. H., Stang, E., and Stenmark, H. (2002) *Nat. Cell Biol.* **4,** 394–398
25. Fisher, R. D., Wang, B., Alam, S. L., Higginson, D. S., Robinson, H., Sundquist, W. I., and Hill, C. P. (2003) *J. Biol. Chem.* **278,** 28976–28984
26. Hofmann, K., and Falquet, L. (2001) *Trends Biochem. Sci.* **26,** 347–350
27. Swanson, K. A., Kang, R. S., Stamenova, S. D., Hicke, L., and Radhakrishnan, I. (2003) *EMBO J.* **22,** 4597–4606
28. Fujiwara, K., Tenno, T., Sugasawa, K., Jee, J. G., Ohki, I., Kojima, C., Tochio, H., Hiroaki, H., Hanaoka, F., and Shirakawa, M. (2004) *J. Biol. Chem.* **279,** 4760–4767
29. Schnell, J. D., and Hicke, L. (2003) *J. Biol. Chem.* **278,** 35857–35860
30. Shih, S. C., Katzmann, D. J., Schnell, J. D., Sutanto, M., Emr, S. D., and Hicke, L. (2002) *Nat. Cell. Biol.* **5,** 389–393
31. Evans, P. C., Ovaa, H., Hamon, M., Kilshaw, P. J., Hamm, S., Bauer, S., Ploegh, H. L., and Smith, T. S. (2004) *Biochem. J.* **378,** 727–734
32. Opipari, A. W., Jr., Boguski, M. S., and Dixit, V. M. (1990) *J. Biol. Chem.* **265,** 14705–14708
33. Davies, B. A., Topp, J. D., Sfeir, A. J., Katzmann, D. J., Carney, D. S., Tall, G. G., Friedberg, A. S., Deng, L., Chen, Z., and Horazdovsky, B. F. (2003) *J. Biol. Chem.* **278,** 19826–19833
34. Polo, S., Sigismund, S., Faretta, M., Guidi, M., Capua, M. R., Bossi, G., Chen, H., De Camilli, P., and Di Fiore, P. P. (2002) *Nature* **416,** 451–455
35. Combet, C., Blanchet, C., Geourjon, C., and Deleage, G. (2000) *Trends Biochem. Sci.* **25,** 147–150